

Depth of a Midcrustal Discontinuity beneath Mt. Vesuvius from the Stacking of Reflected and Converted Waves on Local Earthquake Records

by Vincenzo Nisii,* Aldo Zollo, and Giovanni Iannaccone

Abstract We have developed a technique based on the move-out and stack of reflected seismic phases from local earthquake seismograms. For a given interface depth and a velocity model, the theoretical travel times of reflected/converted phases in a 1D medium are computed and used to align in time the vertical-component microearthquake records collected by a local seismic network. The locations and origin times of events are preliminarily estimated from *P* and *S* arrival times. Different seismic gathers are obtained for each considered reflected/converted phase at that interface, and the best interface depth is chosen as the one that maximizes the value of a semblance function computed on moved-out records.

This method has been applied to seismic records of microearthquakes that occur at Mt. Vesuvius volcano. The analysis confirms the evidence for an 8 to 10-km-deep seismic discontinuity beneath the volcano, which was previously identified, by migration of active seismic data, as the roof of an extended magmatic sill.

Introduction

Reflected and/or converted phases from crustal discontinuities have been observed frequently on microearthquake records (Iyer, 1992). The analysis of secondary arrivals by using different techniques has been proven valuable to define the positions and physical characteristics of reflecting interfaces. The modeling of reflected and/or converted waves is widely used in seismic exploration for retrieving other physical parameters of the propagation medium (*P*-to-*S* impedance contrast, anisotropy, *P*-to-*S* velocity ratio, and so forth) (Yilmaz, 1987; Sheriff and Geldart, 1982).

Recently, studies of wave amplitudes and arrival times of secondary wave trains have been used to delineate the geometry and extension of a magmatic body in various volcanic regions. For example, the location and interpretation, through a travel-time and amplitude analysis, of *S*-to-*S* and *P*-to-*S* reflected phases from a local seismic network in the area of Socorro, Rio Grande rift (New Mexico), has allowed the identification of a sharp crustal discontinuity to a depth of approximately 18 km, interpreted as the top of an extended thin magma layer (Sanford *et al.*, 1973; Rinehart and Sanford, 1981; Balch *et al.*, 1997). Other evidences for mid-crust discontinuities of magmatic origin have been found in Japan at Nikko–Shirane volcano (Matsumoto and Hasegawa, 1996) and in California at Long Valley caldera (Stroujkova and Malin, 2000) from the analysis of *S*-to-*S* and *S*-to-*P* waves observed on microearthquake records.

During the recent past, Mt. Vesuvius volcano has been the target of an extended marine and on-land seismic-exploration program aimed at the high-resolution imaging of the volcanic structure and locating its magmatic feeding system at depth (Zollo *et al.*, 1996; Gasparini *et al.*, 1998; Auger *et al.*, 2001). Detailed 2D tomographic images of the very shallow volcanic structure were obtained from the inversion of first *P* arrivals recorded during an active source experiment in 1996 (Zollo *et al.*, 2002a). A 20- × 20-km² midcrustal seismic reflector was detected at a depth of 8–10 km beneath Mt. Vesuvius volcano by prestack migration of active seismic data, acquired during a dense 2D marine survey in 1997 (Auger *et al.*, 2001). This interface has been interpreted as the top of a thin, very low velocity layer that represents the deep sill-like magmatic reservoir of the volcano.

Since its last eruption in 1944, Mt. Vesuvius has been in a quiescent state characterized by continuous fumarolic and moderate seismic activity. Several hundred microearthquakes per year are detected by the permanent network of Osservatorio Vesuviano (INGV); most events have magnitudes of less than 3 and are located beneath the crater area at rather shallow depths (<4–5 km).

Based on the availability of a high-quality waveform data set, the present study aims at investigating the deep structure of Mt. Vesuvius volcano by the analysis and modeling of reflected/converted phases on microearthquake records. In particular, a relevant target of this study was the possible confirmation of the midcrustal seismic disconti-

*Present address: Osservatorio Vesuviano–Istituto Nazionale di Geofisica e Vulcanologia, Naples, Italy.

nity, which had been already detected by the use of active seismic data.

Mt. Vesuvius is part of a volcanic field within a graben-like structure (the Campanian plain) bordered by Mesozoic limestones. The graben formed during Plio-Pleistocene time and is filled by marine and fluvial sediments interbedded with volcanic products. Information about the shallow structure of the volcano comes primarily from a deep borehole drilled on the southeast slope of Mt. Vesuvius during the 1970s, which penetrates the entire volcanic sequence, having reached Mesozoic limestones at a depth of about 2200 m (Principe *et al.*, 1987). The shallow layer is composed of an interbedded series of Pleistocene volcanic lavas, volcanoclastic and marine–fluvial sedimentary rocks (Di Vito *et al.*, 1999), and it is characterized by P velocities in the range of 1.7–3.3 km/sec (Zollo *et al.*, 2002a). Mesozoic basement P velocities of 5.0–6.0 km/sec are inferred from the P -wave tomographic study (Zollo *et al.*, 2002a) and are consistent with laboratory measurements of well rock samples (Bernard and Zamora, 2000).

In this article the search for deeper discontinuities beneath Mt. Vesuvius is performed by using the move-out and stacking method usually applied in exploration seismology and known as a coherency stack (Naess and Burland, 1985). Based on an *a priori* known background velocity model, the optimal interface depth is found by maximizing the semblance function, computed on the converted and reflected phase signals extracted from the microearthquake records.

Modeling of Reflected/Converted Arrival Times

The proposed method of modeling reflected/converted arrival times follows the approach usually used in reflection seismology to determine the morphology of reflecting interfaces by means of poststack migration of seismic sections.

Assuming a horizontal reflector in a medium with a given 1D background velocity model, the theoretical arrival times of the four possible reflected/converted phases are computed (P -to- P , S -to- P , S -to- S , P -to- S) for any source and receiver pair of the analyzed waveform data set. For each considered wave type, a time window on the seismic records is centered at the theoretical arrival time. The semblance function is computed in the selected time windows for all the records along the entire seismic section. The semblance, S_T , is defined as the ratio of the total energy of the stacked trace in the time interval ($t + \Delta t$) to the sum of the energies of the individual traces in the same time interval (Neidell and Taner, 1971):

$$S_T = \frac{1}{N} \frac{\sum_t \left(\sum_{i=1}^N g_{ti} \right)^2}{\sum_t \sum_{i=1}^N (g_{ti})^2},$$

where g_{ti} is the amplitude of trace i at time t . The semblance

range of variability is between 0 and 1. The semblance is a measure of the waveform similarity between different seismic records. For very coherent events in different records, this function assumes values close to 1. Prior to the computation of the semblance, we normalized the seismic records to minimize the differences arising from varying source magnitudes.

The semblance is evaluated for a given range of interface depths, and for each interface depth different time windows are selected on seismograms according to the newly computed phase arrival times. The optimal interface depth is selected as the one that maximizes the semblance for each of the analyzed reflection and converted events.

Assuming that the background velocity model is correct, a well-identified reflection/conversion event must generate pulses aligned at the zero time value in a moved-out seismic section. The alignment can be quantitatively verified by computing the stack function versus time (i.e., the sum of the amplitude at any time along the seismograms in the entire seismic section). The presence of reflected/converted arrivals in the section will correspond to a peaked stack function, with its maximum at time zero.

The method can be applied for the search of different secondary waves (P -to- P , P -to- S , S -to- P , S -to- S) on three-component seismograms. The comparison of the semblance and stack plots computed for the different phases allows for a better constraint on the interface depth. The method assumes an *a priori* knowledge of the earthquake hypocenters and of the background velocity model, which is assumed to be one dimensional. The uncertainty of these parameters may strongly affect the phase identification in seismograms and the correct positioning of the interface at depth. In addition, other effects can bias the interface location, such as station statics (including topographical effects), and possible 3D heterogeneity of the propagation medium and the irregular morphology of the interface. These parameters and their effect on the final results of our study are discussed later in this article.

Application to Mt. Vesuvius Data

We applied the previously described method to interpret the vertical-component records from 24 local seismic events that occurred between July and December of 1999 and were recorded by the surveillance network operated by Osservatorio Vesuviano, INGV.

The seismic network is composed of 10 seismic stations installed on the flanks of Vesuvius and telemetered to the surveillance center in downtown Naples (Castellano *et al.*, 2002) (Fig. 1). Each station is equipped with a vertical-component, short-period sensor (natural frequency of 1 Hz), and the signal is digitized at a sampling frequency of 100 Hz. Three stations are also equipped with horizontal components. In addition, a temporary network was installed during 1995–1999, composed of four remote digital stations with

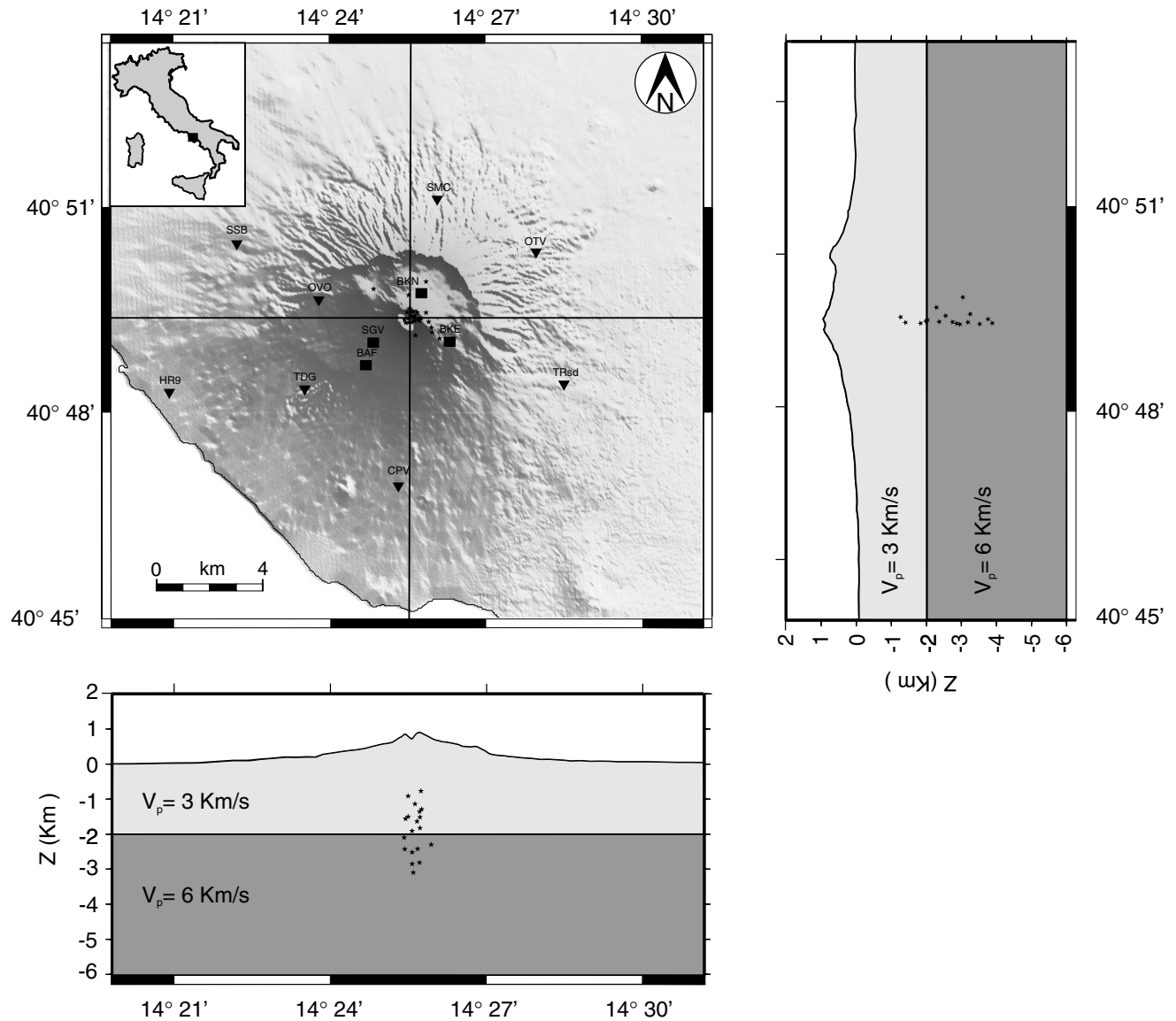


Figure 1. Topographic map showing Mt. Vesuvius and seismic stations of the network owned by Osservatorio Vesuviano, INGV (solid triangles). Temporary stations are indicated by solid squares. The north–south and east–west vertical cross sections show the 24 local-event positions (stars) used in this study and the assumed 1D velocity model.

three-component, short-period seismometers operating in trigger mode.

Twenty-five microearthquakes with duration magnitudes ranging between 0.4 and 3 were selected for the present study, providing 205 vertical-component recordings. The events were located by means of a 3D velocity model, as determined by Lomax *et al.* (2001). The model was obtained by interpolation of 2D tomographic images inferred from the inversion of active seismic arrival-time data (Zollo *et al.*, 2002a). The nonlinear technique proposed by Lomax *et al.* (2000) was used to locate the events. The resulting hypocenters lie along the axial zone of the volcano edifice in a depth range of 1–4 km. The final epicentral distances be-

tween events and stations vary between a few hundred meters to 17 km (Fig. 1). The calculated travel-time rms values are less than 0.1 sec. A time window of 15 sec was chosen for all seismograms, whose origin times have been set according to the value obtained from the earthquake location.

The study of the converted/reflected waves was carried out by considering a reflector depth ranging between 4 and 15 km with a 0.2-km depth interval. A minimum depth value was chosen that is deeper than the discontinuity between the alluvial and recent volcanic sediments and the Mesozoic limestones, whose average depth was determined to be 2 km (Zollo *et al.*, 2002b).

The assumed background velocity model is composed

of one layer over a half-space (Fig. 1). Velocities are assigned according to the average values obtained by the active tomographic study (Zollo *et al.*, 2002a). V_P/V_S is assumed to be uniform and equal to 1.8, according to the estimate of Lomax *et al.* (2001).

The computation of the arrival times of reflected phases was carried out by a two-point ray-tracing technique in a layered velocity model. Only *P-to-P* and *S-to-P* wave types are considered for the analysis, since they are the most readable on vertical-component seismograms. A time window of 0.2 sec centered at the theoretical arrival time of the reflected/converted phase was chosen.

Figure 2 illustrates several examples of recordings in which secondary arrivals are clearly visible. The traces have been aligned at the estimated origin time of microearthquakes. The markers indicate the theoretical arrival times of the direct *S* waves and of the reflected/converted phases (*P-to-P* and *S-to-P*) for an interface at 9 km depth. The recording amplitudes have been normalized to the integral of the absolute value computed along the entire record. This is done to equalize the amplitude among traces to compensate amplitude differences resulting from geometric spreading, magnitude, and radiation pattern. The records have been bandpass filtered between 0.5 and 25 Hz by using a zero-phase-shift Butterworth filter.

The plot of the semblance as a function of the interface depth for the *P-to-P* phase shows two major peaks at about

8 and 9.2 km, the latter being associated with the maximum semblance value (Fig. 3). Two other, smaller peaks are visible at about 6 and 12 km. A similar plot for the *S-to-P* phase shows a maximum semblance at 8.8 km and a secondary peak at about 10.5 km (Fig. 3).

The secondary peaks on both the semblance diagrams could be ambiguously interpreted either as the effect of multiple arrivals at a single interface or of converted/reflected arrivals at interfaces with different depths. This ambiguity can be solved by summing the values of semblance for *P-to-P* and *S-to-P* phases at each interface depth (Fig. 4). In fact, by stacking the semblance values for *P-to-P* and *S-to-P*, the contributions originating at the same interface must sum constructively, thus enhancing the amplitude of the semblance at the corresponding interface depth value.

The normalized stack of *P-to-P* and *S-to-P* semblance curves in Figure 4 shows a well-defined peak for an interface depth of 9 km. As a result of the sum, the small-amplitude, secondary peaks in semblance plots for *P-to-P* and *S-to-P* phases (Fig. 3) have now disappeared, confirming that they were due to the effect of multiple and/or incoherent, small energy arrivals originating at different interfaces.

A smaller amplitude peak at 8 km depth is also detected on the semblance plot of Figure 4. A travel-time difference of about 0.3–0.5 sec is expected for *P-to-P* or *S-to-P* phases originating at interfaces at 8–9 km depth. This time delay is comparable to the uncertainty of semblance estimation, as

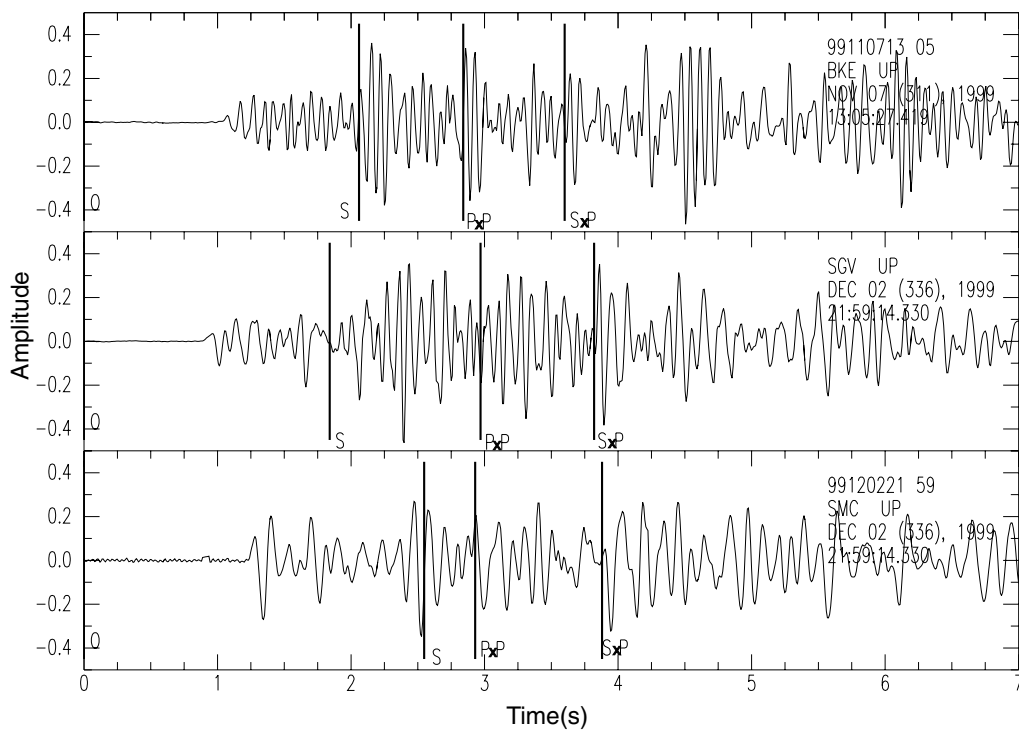


Figure 2. Example of seismograms showing clear secondary arrivals. The zero time is the origin time of the earthquakes. The solid markers indicate the theoretical arrival times of *S* direct waves and of reflected/converted phases *P-to-P* and *S-to-P* from an interface at about 9 km depth.

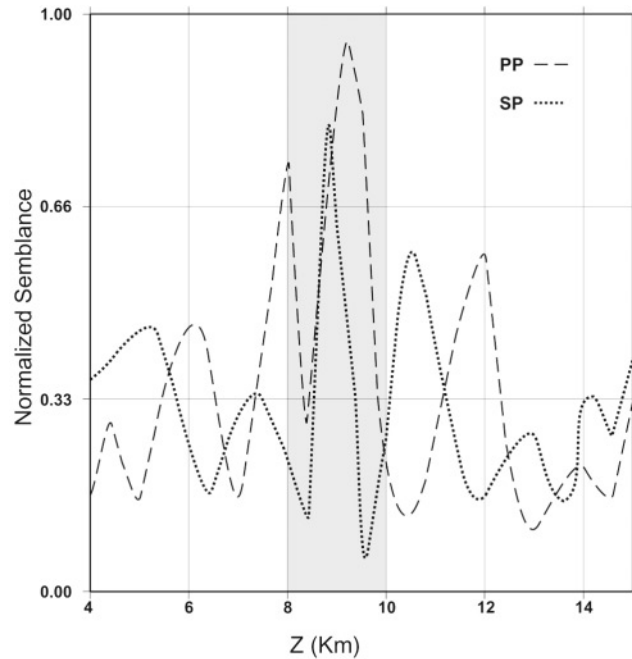


Figure 3. Normalized semblance as a function of reflector depths for reflected/converted phases P -to- P and S -to- P obtained from the seismic record section shown in Figure 5.

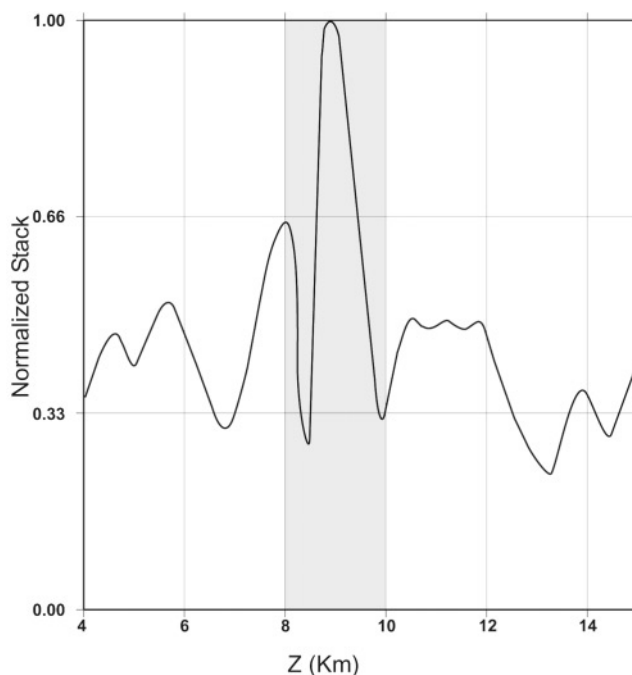


Figure 4. Normalized stack of semblance functions for P -to- P and S -to- P reflected/converted phases of Figure 3.

discussed later, which does not allow us to distinguish between the primary (9 km) and secondary (8 km) peaks. The P -to- P and S -to- P phases identified by the semblance method are clearly visible in seismograms arranged as a common shot gather in a conventional seismic-reflection section (Figs. 5, 6).

The records have been moved out according to the theoretical arrival times of a P -to- P phase for an interface depth of 9 km. The reflected wave pulses align around time zero on the moved-out section in Figure 5. The records of the stack and semblance as a function of time confirm the evidence for a secondary arrival with the presence of a marked peak at time zero. In Figure 6, similar panels for the S -to- P arrival are shown.

The time width of the semblance function around the zero time in Figures 5 and 6 provides a means of quantitatively estimating the uncertainty of the interface depth. Total widths of 0.3 and 0.5 sec are measured for P -to- P and S -to- P phases, respectively. Assuming a velocity of 6 km/sec above the interface, these values suggest an uncertainty of about 1 km for the interface depth.

The main sources of error affecting the width of semblance can be the uncertainty of earthquake location (hypocentral coordinates and origin time), a nonplanar shape of the reflecting interface, or lateral heterogeneity of the velocity model. The peaks at 8- and 9-km depths exhibited in the stacked semblance curve (Fig. 4) therefore can be explained as poorly focused arrivals from the same interface at 8–9-km depth.

Other small peaks of the semblance in the depth ranges of 4–6 km and 10–12 km are observed in the plot in Figure 4. These can be explained as the effect of late, moderate-amplitude arrivals generated by multipathing and scattering of the wave field close to the interface and/or the receiver sites.

In the case of Mt. Vesuvius earthquakes, assuming a realistic variability for all these unknown parameters, the observed variation in the arrival time of reflected/converted phases is much smaller than the average wave travel time from sources to receivers (tenths of a second versus several seconds). This is the reason that, despite the simplicity of the propagation model, one can obtain a satisfactory alignment of the reflected/converted phases, with a small dispersion around the zero time value in the seismic section.

Discussion and Conclusions

The described methodology may be considered a useful tool for identifying and locating the depths of shallow crustal discontinuities when using microearthquake records. The advantage is that, unlike conventional reflection seismics, earthquake sources are located within the investigated medium and have higher energy than active sources. The principal drawback is that the uncertainties of the estimates of source parameters (origin time, source location, fault mech-

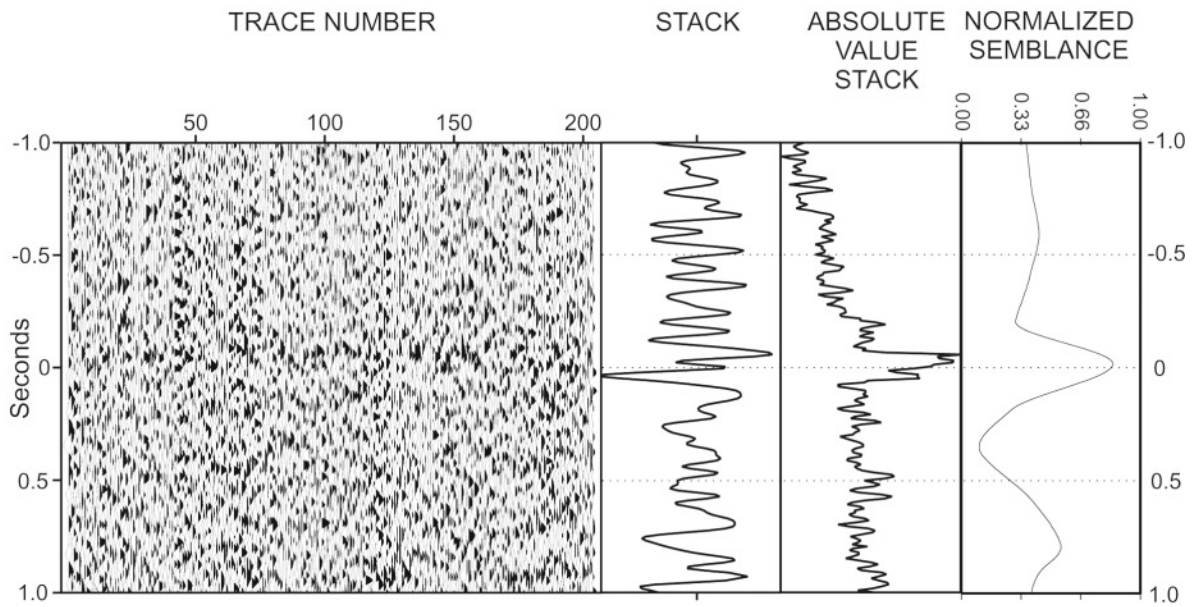


Figure 5. Vertical-component records plotted like a seismic section (gather). Note the *P-to-P* reflected phases from a 9-km-depth reflecting interface at about zero time. The stack of absolute values of the records is a good qualitative indicator of energy content in the section, because it avoids loss from different polarities of the seismic phases.

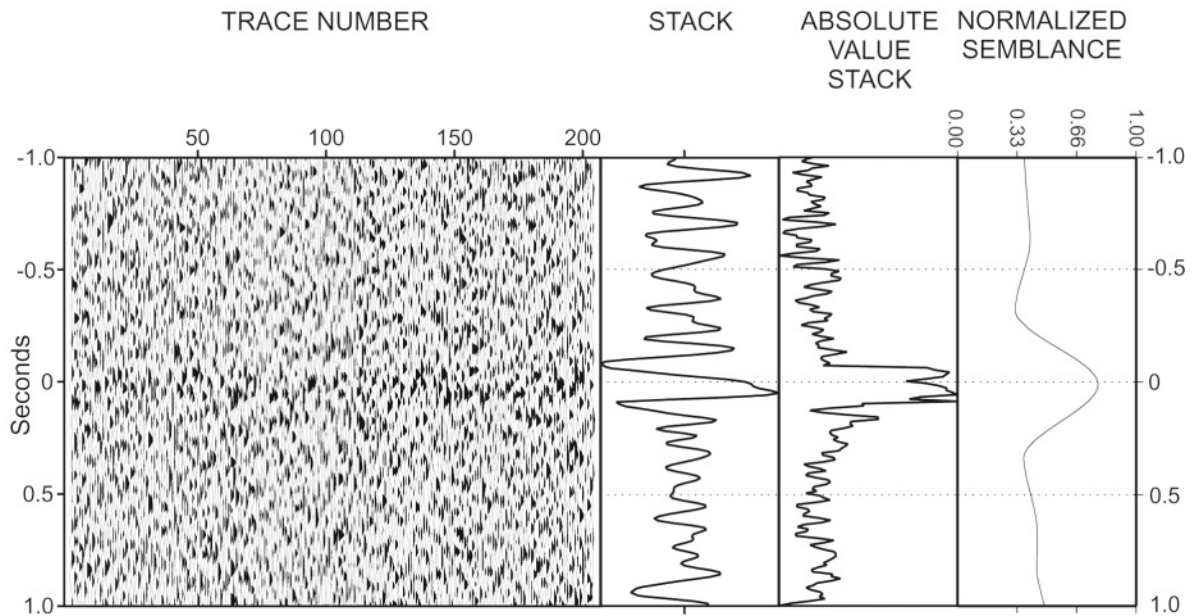


Figure 6. Vertical-component records plotted like a seismic section (gather). Note the *S-to-P* reflected phases from a 9-km-depth reflecting interface at about zero time. The stack of absolute values of the records is a good qualitative indicator of energy content in the section, because it avoids loss from different polarities of the seismic phases.

anism) can influence the quality of the stack, thus affecting the accuracy of the interface depth.

Despite the assumed simplicity of the propagation medium, the technique has proven to be robust and efficient for the search and first-order modeling of secondary arrivals on

microearthquake records. The shape and width of the semblance function peak is a measure of the uncertainty of the interface depth, since a narrow semblance curve indicates a well-constrained interface depth. It also provides an estimate for the phase-timing error (about 0.3 and 0.5 for *P-to-P* and

S-to-*P* phases, respectively), which is related to unknown path and source effects. We applied this methodology to *P*-to-*P* and *S*-to-*P* waves observed on local earthquake records acquired by the surveillance seismic network operating on Mt. Vesuvius volcano.

Recent studies of crustal discontinuities beneath Mt. Vesuvius volcano by using the reflected/converted wave field were performed by Auger *et al.* (2001) using an active seismic data set. Based on the modeling of wave amplitudes as a function of the incidence angle, these authors identified a major seismic discontinuity at about 8 km depth, characterized by a negative velocity contrast (from 6 to less than 4 km/sec for *P* waves and from 3.5 to less than 1 km/sec for *S* waves).

Our analysis of microearthquake records confirms this evidence but provides a slightly greater value for the interface depth (9 km) beneath the volcanic complex. This discrepancy can be attributed to the use of a simplified crustal model, whereas in the Auger *et al.* study, accurate static corrections have been applied to data to account for the lateral variation of the shallow velocity structure.

Based on the measured velocity contrast, Auger *et al.* interpreted the reflector as the top of a midcrust, sill-like magmatic reservoir beneath the volcanic complex, having a lateral extent of at least 400 km². The hypothesis for a deep magmatic reservoir beneath Mt. Vesuvius is also supported by the evidence for a highly conductive zone between 8 and 10 km depth, which was identified by 1D magnetotelluric profiles (Di Maio *et al.*, 1998). Moreover, the fluid-inclusion analysis of minerals contained in Mt. Vesuvius eruptive products indicates a formation depth between 4 and 10 km (Belkin and De Vivo, 1993).

The thickness of the midcrustal sill is not accurately known, but it could be in the range of 0.5–2.0 km, which is consistent with the dominant reflection phase frequencies and the available estimates of the volume of erupted magma (more than 50 km³), considering that this represents only slightly less than 30% of the stored magma volume. Isotopic-ratio analysis of lava samples indicates long residence times of magma in a mid-crust reservoir with contamination from continental crustal rocks (Civetta *et al.*, 2004). This result, and the *P* and *S* velocities estimated by Auger *et al.* (2001), suggest a partially molten body, consistent with a highly fractured rock with diffusive melt.

Several observations of midcrust discontinuities associated with magmatic reservoirs beneath volcanoes have been made worldwide, based on seismic-data modeling. Beneath the Nikko–Shirane volcano (Northeast Japan arc) a midcrust reflector was identified at 8–15 km depth with a lateral extension of about 15 × 15 km², which is interpreted as the top of a low-velocity thin layer of partial-melt material (Matsumoto and Hasegawa 1996). In the volcanic area of Casa Diablo, Long Valley, California, seismic reflections from a 1.5- × 2-km² curved surface have been interpreted as produced by the roof of a magma chamber at about 7.8 km depth by Sanders (1984).

The presence of magmatic sills in the depth range of 8–20 km beneath different volcanoes worldwide is attributed to a neutral condition of the magma buoyancy force with the surrounding crust. The uprising of magma from the mantle in an extensional tectonic regime can give rise to thin and wide sill reservoirs in the upper crust (Ryan, 1994; Iyer *et al.*, 1990).

The discovery of a deep, sill-like magmatic reservoir beneath Mt. Vesuvius is relevant for the understanding and modeling of possible future eruptive scenarios. The existence of a smaller size (0.01–0.02 km³), shallow (less than 3 km depth) magmatic reservoir was previously suggested by geochemical and petrological analyses of products ejected during the most recent eruptions (1906, 1944) (Civetta and Santacroce, 1992; Marianelli *et al.*, 1999), although no seismic signature of shallow volumes of molten materials has been found from high-resolution seismic exploration surveys (Zollo *et al.*, 2002a). The possible connection and interaction between deep and shallow magmatic sources during future eruptive unrest at Mt. Vesuvius is currently under discussion. Further geophysical investigation is needed to ascertain the lateral extent and thickness of the magma sill in order to have reliable estimates of the potential amount of magma available for the next eruption.

Acknowledgments

E. Auger and L. D'Auria are acknowledged for their useful comments and suggestions. The comments and suggestions of C. Rowe (editor) and of two anonymous reviewers helped to improve the quality and clarity of the article. The present work was supported by Gruppo Nazionale di Vulcanologia (INGV), Framework Program 2000–2003.

References

- Auger, E., P. Gasparini, J. Virieux, and A. Zollo (2001). Imaging of a mid-crust high to low seismic discontinuity beneath Mt. Vesuvius, *Science* **204**, 1510–1512.
- Balch, R. S., H. E. Hartse, A. Sanford, and K. Lin (1997). A new map of the geographic extent of the Socorro mid-crustal magma body, *Bull. Seism. Soc. Am.* **87**, 174–182.
- Belkin, H. E., and B. De Vivo (1993). Fluid inclusion studies of ejected nodules from plinian eruptions of Mt. Vesuvius, *J. Volcanol. Geother. Res.* **58**, 89–100.
- Bernard, M.-L., and M. Zamora (2000). Mechanical properties of volcanic rocks and their relations to transport properties, *EOS* **81**, Fall Meet. Suppl., Abstract V71A-33.
- Castellano, M., C. Buonocunto, M. Capello, and M. La Rocca (2002). Seismic surveillance of active volcanoes: the Osservatorio Vesuviano Seismic Network (OVSN—Southern Italy), *Seism. Res. Lett.* **73**, 177–184.
- Civetta, L., and R. Santacroce (1992). Steady-state magma supply in the last 3400 years of Vesuvian activity, *Acta Volcanol.* **2**, 147–159.
- Civetta, L., M. D'Antonio, S. de Lorenzo, V. Di Renzo, and P. Gasparini (2004). Thermal and geochemical constraints on the “deep” magmatic structure of Mt. Vesuvius, *J. Volcanol. Geother. Res.* **133** (1–4), 1–12.
- Di Maio, R., P. Mauriello, D. Patella, Z. Petrillo, S. Piscitelli, and A. Siniscalchi (1998). Electric and electromagnetic outline of the Mount Somma–Vesuvius structural setting, *J. Volcanol. Geother. Res.* **82**, 219–238.
- Di Vito, M. A., R. Sulpizio, G. Zanchetta, and G. Calderoni (1999). The

- geology of south western slopes of Somma–Vesuvius, Italy, as inferred by borehole stratigraphies and cores, *Acta Vulcanol.* **10**, 383–393.
- Gasparini, P., and Tomoves Working Group (1998). Looking inside Mount Vesuvius, *EOS* **79**, 229–232.
- Iyer, H. M. (1992). Seismological detection and delineation of magma chambers: present status with emphasis on the western USA, in *Volcanic Seismology*, P. Gasparini, R. Scarpa, and K. Aki (Editors), Springer-Verlag, New York, 299–338.
- Iyer, H. M., J. R. Evans, P. B. Dawson, D. A. Stauber, and U. Achauer (1990). Differences in magma storage in different volcanic environments as revealed by seismic tomography: silicic volcanic centers and subduction-related volcanoes, in *Magma Transport and Storage*, M. P. Ryan (Editor), Wiley, New York, 293–316.
- Lomax, A., J. Virieux, P. Volantand, and C. Berge (2000). Probabilistic earthquake location in 3D and layered models: introduction to a Metropolis–Gibbs method and comparison with linear locations, in *Advances in Seismic Event Location*, C. H. Thurber and N. Rabinowitz (Editors), Kluwer, Amsterdam, 101–134.
- Lomax, A., A. Zollo, P. Capuano, and J. Virieux (2001). Precise, absolute earthquake location under Somma–Vesuvius volcano using a new 3D velocity model, *Geophys. J. Int.* **146**, 313–331.
- Marianelli, P., N. Metrich, and A. Sbrana (1999). Shallow and deep reservoir involved in the magma supply of the 1944 eruption of Vesuvius, *Bull. Volcanol.* **61**, 48–63.
- Matsumoto, S., and A. Hasegawa (1996). Distinct *S* wave reflector in the midcrust beneath Nikko–Shirane volcano in the northeastern Japan arc, *J. Geophys. Res.* **101**, 3067–3083.
- Naess, O. E., and L. Bruland (1985). Stacking methods other than simple summation, in *Developments in Geophysical Methods 6*, A. A. Fitch (Editor), Elsevier Science London, 189–223.
- Neidell, N. S., and M. S. Taner (1971). Semblance and other coherency measurements for multichannel data, *Geophysics* **36**, 482–497.
- Principe, C., M. Rosi, R. Santacroce, and A. Sbrana (1987). Geophysics, in *Somma-Vesuvius*, R. Santacroce (Editor), CNR Editions, Rome, 11–52.
- Rinehart, E., and A. R. Sanford (1981). Upper crustal structure of the Rio Grande Rift near Socorro, New Mexico, from inversion of microearthquake *S*-wave reflections, *Bull. Seism. Soc. Am.* **71**, 437–450.
- Ryan, M. P. (1994). Neutral-buoyancy controlled magma transport and storage in mid-ocean ridge magma reservoirs and their sheeted-dike complex: a summary of basic relationships, in *Magmatic Systems*, M. P. Ryan (Editor), Vol. 2, Academic, London, 97–138.
- Sanders, C. O. (1984). Location and configuration of magma bodies beneath Long Valley, California, determined from anomalous earthquake signals, *J. Geophys. Res.* **89**, 8287–8302.
- Sanford, A. R., O. Alptekinand, and T. R. Toppozada (1973). Use of reflection phases on microearthquake seismograms to map an unusual discontinuity beneath the Rio Grande Rift, *Bull. Seism. Soc. Am.* **63**, 2021–2034.
- Sheriff, R. E., and L. P. Geldart (1982). *Exploration Seismology* (in 2 Vol.), Cambridge Univ. Press, New York.
- Stroujkova, A. F., and P. E. Malin (2000). A magma mass beneath Casa Diablo? Further evidence from reflected seismic waves, *Bull. Seism. Soc. Am.* **90**, 500–511.
- Yilmaz, O. (1987). Seismic data processing, in *Investigations in Geophysics*, B. Nictzel (Editor), Vol. 2, Soc. Expl. Geophys. Tulsa, Oklahoma.
- Zollo, A., P. Gasparini, J. Virieux, H. Le Meur, G. De Natale, G. Biella, E. Boschi, P. Capuano, R. de Franco, P. Dell’Aversana, R. De Matteis, I. Guerra, G. Iannaccone, L. Mirabileand, and G. Vilardo (1996). Seismic evidence for a low-velocity zone in the upper crust beneath Mount Vesuvius, *Science* **274**, 592–594.
- Zollo, A., L. D’Auria, R. De Matteis, A. Herrero, J. Virieux, and P. Gasparini (2002a). Bayesian estimation of 2-D *P*-velocity models from active seismic arrival time data: imaging of the shallow structure of Mt. Vesuvius (southern Italy), *Geophys. J. Int.* **151**, 556–582.
- Zollo, A., W. Marzocchi, P. Capuano, A. Lomax, and G. Iannaccone (2002b). Space and time behaviour of seismic activity at Mt. Vesuvius volcano, southern Italy, *Bull. Seism. Soc. Am.* **92**, 625–640.
- Osservatorio Vesuviano (INGV)
Via Diocleziano 328, 80124
Naples, Italy
(INGV)
- Dipartimento di Scienze Fisiche
Università degli Studi di Napoli “Federico II”
Complesso Univ. Monte S. Angelo
Via Cinthia, 80125
Naples, Italy
aldo.zollo@na.infn.it
(A.Z.)

Manuscript received 10 April 2003.